Synthesis and Characterization of Dinuclear Ruthenium Complexes with Tetra-2-pyridylpyrazine as a Bridge

Chris M. Hartshorn,[†] Nadime Daire,[‡] Valerie Tondreau,[‡] Barbara Loeb,[‡] Thomas J. Meyer,*[,†] and Peter S. White[†]

Department of Chemistry, CB#3290, Venable Hall, The University of North Carolina, Chapel Hill, North Carolina 27599-3290, and Facultad de Quimica, P. Universidad Católica de Chile, Casilla 306, Santiago, Chile

Received January 26, 1999

The syntheses and characterization of a series of complexes of the general formula [Cl(bpy′)Ru(tppz)Ru(bpy′)-Cl](PF$_6$)$_2$, where tppz is tetra-2-pyridylpyrazine and bpy′ is 2,2′-bipyridine or substituted 2,2′-bipyridine, are described. Preparations with 2,2′-bipyridine or 4,4′-dimethyl-2,2′-bipyridine (**1** and **2**, respectively) give mixtures of two isomers. The isomers of **2** were separated chromatographically and the X-ray crystal structure of the cis isomer was solved. Significant distortion is observed in both the coordination geometry around each ruthenium atom and in the tppz ligand resulting in short intramolecular Ru···Ru and Cl···Cl separations (6.558(1) and 5.880-(2) Å, respectively). Ligands containing two bipyridine groups linked through eight- and nine-atom bridges have also been synthesized. The length of the bridge between bipyridine groups allows for the formation of cis complexes **3**−**5** having the general formula shown above but prevents formation of a trans isomer.

Introduction

An extensive array of high oxidation state ruthenium−oxo complexes have previously been synthesized and their reactivity with organic and inorganic substrates investigated.[1−19] Relatively few of these have incorporated more than one ruthenium center into a single complex despite the observation of novel reactivity in such complexes, most notably in water oxidation by the "blue dimer", *cis*,*cis*-[(bpy)$_2$(H$_2$O)Ru^{III}ORu^{III}(H$_2$O)(bpy)$_2$]$^{4+}$.[20−27] We are interested in the reactivity properties of ligand-bridged dinuclear complexes where there may be cooperative features in addition to the reactivity of the individual sites. To this end we are developing synthetic methodologies and investigating the properties of a series of complexes containing ruthenium bridged by the pyrazine-derivative 2,3,5,6-tetra-2-pyridylpyrazine (tppz).

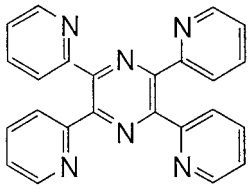

tppz

Complexes of this ligand have been investigated, most recently by Abruña et al.,[28] Brewer et al.,[29] and Sauvage et al.,[30] in which redox, luminescence, and mixed-valence properties of ruthenium and osmium complexes were reported. In these cases, Ru^{II} or Os^{II} coordinated to tppz were "capped" by tridentate ligands to occupy the remaining coordination sites. In preparing potential oxo precursors, one coordination site is required for the introduction of an aqua ligand with sequential oxidation and proton loss, as in eq 1, to give the Ru^{IV}-oxo form.

[†] University of North Carolina at Chapel Hill.
[‡] P. Universidad Católica de Chile.

(1) Stultz, L. K.; Binstead, R. A.; Reynolds, M. S.; Meyer, T. J. *J. Am. Chem. Soc.* **1995**, *117*, 2520.
(2) Cheng, W.-C.; Yu, W.-Y.; Cheung, K.-K.; Che, C.-M. *J. Chem. Soc., Chem. Commun.* **1994**, 1063.
(3) Dovletoglou, A.; Meyer, T. J. *J. Am. Chem. Soc.* **1994**, *116*, 215.
(4) Cheng, W.-C.; Yu, W.-Y.; Cheung, K.-K.; Che, C.-M. *J. Chem. Soc., Dalton Trans.* **1994**, 57.
(5) Binstead, R. A.; McGuire, M. E.; Dovletoglou, A.; Seok, W. K.; Roecker, L.; Meyer, T. J. *J. Am. Chem. Soc.* **1992**, *114*, 173.
(6) Seok, W. K.; Meyer, T. J. *J. Am. Chem. Soc.* **1988**, *110*, 7358.
(7) Roecker, L.; Meyer, T. J. *J. Am. Chem. Soc.* **1987**, *109*, 746.
(8) Marmion, M. E.; Takeuchi, K. J. *J. Am. Chem. Soc.* **1988**, *110*, 1472.
(9) Marmion, M. E.; Takeuchi, K. J. *J. Am. Chem. Soc.* **1986**, *108*, 510.
(10) Thompson, M. S.; Meyer, T. J. *J. Am. Chem. Soc.* **1982**, *104*, 4106.
(11) Thompson, M. S.; Meyer, T. J. *J. Am. Chem. Soc.* **1982**, *104*, 5070.
(12) Thompson, M. S.; DeGiovani, W. F.; Moyer, B. A.; Meyer, T. J. *J. Org. Chem.* **1984**, *25*, 4972.
(13) Thompson, M. S.; DeGiovani, W. F.; Moyer, B. A.; Meyer, T. J. *J. Am. Chem. Soc.* **1980**, *102*, 2310.
(14) Che, C. M.; Yam, V. W. W. *Adv. Inorg. Chem.* **1992**, *39*, 233.
(15) Nugent, W. A.; Mayer, J. M. *Metal−Ligand Multiple Bonds*; Wiley: New York, 1988.
(16) Meyer, T. J. In *Metal Oxo Complexes and Oxygen Activation*; Martell, A. E., Ed.; Plenum: New York, 1988; pp 33−47.
(17) Holm, R. H. *Chem. Rev.* **1987**, *87*, 1401.
(18) Gulliver, D. J.; Levason, W. *Coord. Chem. Rev.* **1982**, *46*, 1.
(19) Sheldon, R. A.; Kochi, J. K. *Metal-Catalyzed Oxidations of Organic Compounds*; Academic: New York, 1981.
(20) Chronister, C. W.; Binstead, R. A.; Meyer, T. J. *Inorg. Chem.* **1997**, *36*, 3814.
(21) Lei, Y.; Hurst, J. K. *Inorg. Chim. Acta* **1994**, *226*, 179.
(22) Lei, Y.; Hurst, J. K. *Inorg. Chem.* **1994**, *33*, 4460.
(23) Hurst, J. K.; Zhou, J.; Lei, Y. *Inorg. Chem.* **1992**, *31*, 1010.
(24) Geselowitz, D.; Meyer, T. J. *Inorg. Chem.* **1990**, *29*, 3894.
(25) Raven, S. J.; Meyer, T. J. *Inorg. Chem.* **1988**, *27*, 4478.
(26) Gilbert, J. A.; Eggleston, D. S.; Murphy, W. R.; Geselowitz, D. A.; Gersten, S. W.; Hodgson, D. J.; Meyer, T. J. *J. Am. Chem. Soc.* **1985**, *107*, 3855.
(27) Gersten, S. W.; Samuels, G. J.; Meyer, T. J. *J. Am. Chem. Soc.* **1982**, *104*, 4029.
(28) Arana, C. R.; Abruña, H. D. *Inorg. Chem.* **1993**, *32*, 194.
(29) Vogler, L. M.; Brewer, K. J. *Inorg. Chem.* **1996**, *35*, 818.
(30) Collin, J.-P.; Lainé, P.; Launay, J.-P.; Sauvage, J.-P.; Sour, A *J. Chem. Soc., Chem. Commun.* **1993**, 435.

10.1021/ic990110a CCC: $18.00 © 1999 American Chemical Society
Published on Web 05/29/1999

$$cis\text{-}Ru^{II}(bpy)_2(py)(H_2O)^{2+} \underset{+e^-,\,+H^+}{\overset{-e^-,\,-H^+}{\rightleftharpoons}} cis\text{-}Ru^{III}(bpy)_2(py)(OH)^{2+} \underset{+e^-,\,+H^+}{\overset{-e^-,\,-H^+}{\rightleftharpoons}} cis\text{-}Ru^{IV}(bpy)_2(py)(O)^{2+} \quad (1)$$

In a previous report, the crystal structure of the mononuclear complex [Ru(tppz)(dmb)Cl]PF_6 (dmb = 4,4′-dimethylbipyridine), synthesized by reaction of [Ru(dmb)Cl_4] with tppz, was reported.[31] An approach to analogous dinuclear complexes having an available coordination site at each ruthenium is to utilize the precursor [Cl_3Ru(tppz)RuCl_3] and allow this to react with bpy to give [Cl(bpy)Ru(tppz)Ru(bpy)Cl]$(PF_6)_2$ followed by substitution of Cl^- by known procedures. Although feasible, this approach introduces the complication of cis and trans isomers as illustrated in Figure 1.

Given the considerable difference in relative spatial disposition of the Ru−Cl sites across the bridge for the two isomers, large differences are expected in the cooperative reactivity of the oxo groups if the di-oxo forms can be prepared.

We report here the preparation and properties of the isomeric mixtures *cis*/*trans*-[Cl(bpy)Ru(tppz)Ru(bpy)Cl]$(PF_6)_2$ (**1**), *cis*/*trans*-[Cl(dmb)Ru(tppz)Ru(dmb)Cl]$(PF_6)_2$ (**2**), and of *cis*-**2** and *trans*-**2** which have been separated chromatographically. We also report the synthesis and properties of the series of "strapped" ligand-bridged complexes **3**−**5** (Figure 1) in which the geometry across the tppz bridge is constrained to be cis. Their use as *cis*-directed oxidants could be important given the time-consuming procedures required for isomeric separation of **2**.

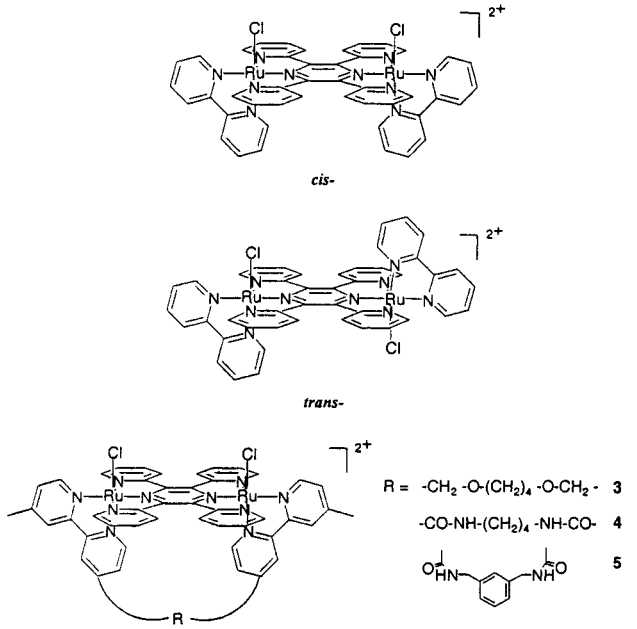

Figure 1. Cis (top) and trans (middle) isomers of [Cl(bpy)Ru(tppz)-Ru(bpy)Cl]$^{2+}$ and "strapped" complexes **3**−**5** (bottom).

Experimental Procedures

Materials. Solvents and reagents were obtained from commercial sources and used as received. 4-Hydroxymethyl-4′-methyl-2,2′-bipyridine and 4′-methyl-2.2′-bipyridine-4-carboxylic acid were prepared according to literature procedures.[32,33] The tppz bridging ligand was prepared by literature procedures,[34] and also purchased from G. F. Smith.

Instrumentation. ^{1}H NMR spectra were recorded on Varian Gemini 300 MHz or Bruker AC/200 200 MHz spectrometers fitted with a 5-mm probe. Spectra recorded in $CDCl_3$ were referenced relative to an internal $SiMe_4$ standard, while those recorded in DMSO-d_6 and CD_3CN were referenced to solvent resonances. UV−visible spectra were recorded by using Hewlett-Packard 8452A diode array or Milton Roy 3000 diode array spectrophotometers. Electrochemical measurements were conducted in CH_3CN, 0.1 M in ($N(n\text{-}C_4H_9)_4$)PF_6 (TBAH) as electrolyte with a PAR model 273 potentiostat. A 2-mm diameter polished glassy carbon disk was the working electrode, a Ag/$AgNO_3$ electrode, standardized against ferrocene, as the reference and a platinum wire as the auxiliary electrode. A two-compartment cell was used with a sintered glass disk separating the compartment containing the reference electrode from that containing the working and auxiliary electrodes. Microanalyses were performed by Oneida Research Services.

Syntheses. 1,4-Bis(4′-methyl-2,2′-bipyridyl-4-methoxy)butane (6). 1,4-Dibromobutane (0.75 mmol), 4-hydroxymethyl-4′-methyl-2,2′-bipyridine (1.50 mmol), and potassium hydroxide (7.5 mmol) were heated at reflux in toluene (10 mL) for 21 h. The reaction mixture was concentrated under reduced pressure, and the remaining residue was separated between chloroform (10 mL) and water (10 mL). The organic layer was dried (Na_2SO_4) and concentrated under reduced pressure yielding the crude product as an off-white solid. Recrystallization from hexane/chloroform (20:1) gave **6** as a white solid (61% yield). ^{1}H NMR ($CDCl_3$, δ): 1.77, 4H, t, 2,3-CH_2; 2.43, 6H, s, CH_3; 3.56, 4H, t, 1,4-CH_2; 4.59, 4H, s, O-CH_2-bpy; 7.13, 2H, d, H5′; 7.33, 2H, d, H5; 8.23, 2H, s, H3′; 8.31, 2H, s, H3; 8.52, 2H, d, H6′; 8.62, 2H, d, H6. Anal. Calcd for $C_{28}H_{30}N_4O_2$: C, 73.98; H, 6.65; N, 12.32. Found: C, 73.82; H, 6.78; N, 12.04.

1,4-Bis(4′-methyl-2,2′-bipyridyl-4-carbonylamino)butane (7). 1,4-Diaminobutane (1.93 mmol), 4′-methyl-2.2′-bipyridine-4-carboxylic acid (7.72 mmol), (1-benzotriazoleoxy)tris(dimethylamino)phosphonium hexafluorophosphate (BOP, 7.72 mmol), 1-hydroxybenzotriazole (HOBt, 7.72 mmol), *N*-methylmorpholine (NMM, 11.58 mmol), and 4-(dimethylamino)pyridine (DMAP, 1.15 mmol) were stirred in DMF (40 mL) at 50 °C for 19 h. A precipitate formed in the reaction mixture which, upon cooling, was collected and washed with hot chloroform (3 × 10 mL) and diethyl ether (3 × 10 mL) to give **7** as a white solid (87% yield). ^{1}H NMR (DMSO-d_6, δ): 1.62, 4H, t, 2,3-CH_2; 2.42, 6H, s, CH_3; 3.38, 4H, q, 1,4-CH_2; 7.32, 2H, d, H5′; 7.79, 2H, d, H5; 8.26, 2H, s, H3′; 8.57, 2H, s, H6′; 8.75, 2H, d, H3; 8.79, 2H, d, H6; 8.94, 2H, t, NH. Anal. Calcd for $C_{28}H_{28}N_6O_2$: C, 69.98; H, 5.87; N, 17.49. Found: C, 70.19; H, 5.78; N. 17.32.

1,3-Bis(4′-methyl-2,2′-bipyridyl-4-carbonylaminomethyl)-benzene (8). 1,3-Bis(amino-methyl)benzene (1.28 mmol), 4′-methyl-2.2′-bipyridine-4-carboxylic acid (5.12 mmol), BOP (5.12 mmol), HOBt (5.12 mmol), NMM (7.68 mmol), and DMAP (0.76 mmol) were stirred in DMF (30 mL) at 50 °C for 24 h. The reaction mixture was concentrated under high vacuum and the remaining residue suspended in chloroform/ethyl acetate (1:2, 100 mL). The suspension was washed with water (2 × 30 mL), sodium hydroxide (1 M, 3 × 30 mL), and water (2 × 30 mL). Filtering at this point gave a small amount of **8** (approximately 30% yield). Concentration of the organic phase gives further **8** as a pure white solid (overall yield 91%). ^{1}H NMR (DMSO-d_6, δ): 2.41, 6H, s, CH_3; 3.50, 4H, d, CH_2; 7.22−7.31, 6H, m, H5′, C_6H_4; 7.79, 2H, d, H5; 8.23, 2H, s, H3′; 8.52, 2H, s, H6′; 8.75, 2H, d, H6; 8.76, 2H, d, H3; 9.50, 2H, t, NH. Anal. Calcd for $C_{32}H_{28}N_6O_2$: C, 72.71; H, 5.34; N, 15.90. Found: C, 72.35; H, 5.62; N, 15.63.

[Cl_3Ru(tppz)RuCl_3]. Ruthenium(III) chloride hydrate (0.3 g) and tppz (0.15 g) were heated at reflux in ethanol (100 mL) under argon for 3 h. The reaction mixture was cooled to room temperature and filtered. The solid obtained was washed with ether and used for subsequent reactions without purification.

General Procedure for *cis*/*trans*-bpy/tppz Complexes 1 and 2. [Cl_3Ru(tppz)RuCl_3] (0.31 mmol), 4,4′-Rbpy (0.93 mmol) (R = H, CH_3), lithium chloride (3 mmol), and triethylamine (0.4 mL) were heated at

(31) Tondreau, V.; Leiva, A. M.; Loeb, B.; Boys, D.; Stultz, L. K.; Meyer, T. J. *Polyhedron* **1996**, *15*, 2035.
(32) Furue, M.; Yoshidzumi, S.; Kinoshita, S.; Kushida, T.; Nozakura, S.; Kamachi M. *Bull. Chem. Soc. Jpn* **1991**, *64*, 1632.
(33) Peek, B. M.; Ross, G. T.; Edwards, S. W.; Meyer, G. J.; Meyer, T. J.; Erickson, B. W. *Int. J. Peptide Protein Res.* **1991**, *38*, 114.
(34) Goodwin, H. A.; Lyons, F. *J. Am. Chem. Soc.* **1959**, *81*, 6415.

reflux in ethanol/water (3:1, 60 mL) under argon for 6 h. The ethanol was removed under reduced pressure and aqueous ammonium hexafluorophosphate added, giving a dark green precipitate. The residue was purified by alumina chromatography to give the product as a dark green solid.

***cis/trans*-[Cl(bpy)Ru(tppz)Ru(bpy)Cl](PF$_6$)$_2$ (1).** Eluting with toluene/acetonitrile (1:3) gave **1** (57% yield). ^{1}H NMR (CD_3CN, δ): 6.98−8.85, 30H; 10.15, 10.26, 2H, d, H6″. Anal. Calcd for $C_{44}H_{32}N_{10}Cl_2F_{12}P_2Ru_2$: C, 41.82; H, 2.55; N, 11.08. Found: C, 41.55; H, 2.43; N. 10.72.

***trans*-[Cl(dmb)Ru(tppz)Ru(dmb)Cl](PF$_6$)$_2$ (*trans*-2) and *cis*-[Cl(dmb)Ru(tppz)Ru(dmb)Cl](PF$_6$)$_2$ (*cis*-2).** The isomeric mixture was first isolated from the crude product by eluting with toluene/acetonitrile (2:3) (64% yield). No separation of *trans*-**2** and *cis*-**2** was observed. Anal. Calcd for $C_{48}H_{40}N_{10}Cl_2F_{12}P_2Ru_2$: C, 43.68; H, 3.05; N, 10.61. Found: C, 43.33; H, 2.82; N, 10.18. A small amount of this isomeric mixture was loaded on to a second alumina column and eluted with toluene/acetonitrile (1:1) by using a slow eluent flow rate. *trans*-**2** eluted from the column first, followed by *cis*-**2**, the collection of which was completed by eluting with toluene/acetonitrile (1:3). *trans*-**2**: ^{1}H NMR (CD_3CN, δ): 2.34, 6H, s, CH_3; 2.82, 6H, s, CH_3; 6.83, 2H, d, H5′; 7.01, 2H, d, H6′; 7.46, 4H, t, H4; 7.86, 4H, t, H5; 7.91, 2H, d, H5″; 7.94, 4H, d, H3; 8.27, 2H, s, H3′; 8.58, 2H, s, H3″; 8.77, 4H, d, H6; 10.04, 2H, d, H6″. *cis*-**2**: ^{1}H NMR (CD_3CN, δ): 2.43, 6H, s, CH_3; 2.83, 6H, s, CH_3; 6.94, 2H, d, H5′; 7.45, 4H, t, H4; 7.59, 2H, d, H6′; 7.83−7.92, 10H, m, H5, H5″, H3; 8.34, 2H, s, H3′; 8.63, 2H, s, H3″; 8.77, 4H, d, H6; 9.93, 2H, d, H6″.

General Procedure for Bridged *cis*-bpy/tppz Complexes 3−5. [Cl_3Ru(tppz)RuCl_3] (0.15 mmol), (4′-Me-bpy-4-)$_2$R (0.15 mmol), lithium chloride (1.5 mmol), and triethylamine (0.4 mL) were heated at reflux in ethanol/water (3:1, 120 mL) under argon for 6 h. The ethanol was removed under reduced pressure and aqueous ammonium hexaflourophosphate added giving a dark green precipitate. The residue was purified by alumina chromatography to give the product as a dark green solid.

Ether/tppz Bridged Complex (3) (R = -CH$_2$-O-(CH$_2$)$_4$-O-CH$_2$-). Eluting with toluene/acetonitrile (starting with 50% acetonitrile and increasing slowly to 100%) gave **3** (18% yield). ^{1}H NMR (CD_3CN, δ): 1.57, 4H, t, 2,3-CH_2; 2.83, 6H, s, CH_3; 3.44, 4H, t, 1,4-CH_2; 4.59, 4H, s, O−CH_2-bpy; 6.91, 2H, d, H6′; 7.20, 2H, d, H5′; 7.54, 4H, t, H4; 7.90, 4H, t, H5; 8.00, 2H, d, H5″; 8.08, 4H, br, H3; 8.18, 2H, s, H3′; 8.51, 2H, s, H3″; 8.82, 4H, d, H6; 10.15, 2H, d, H6″. Anal. Calcd for $C_{52}H_{46}N_{10}Cl_2F_{12}O_2P_2Ru_2$: C, 44.42; H, 3.30; N, 9.96. Found: C, 44.51; H, 3.08; N, 9.86.

Butyldiamide/tppz Bridged Complex (4) (R = -CO-NH-(CH$_2$)$_4$-NH-CO-). Eluting with acetonitrile gave **4** (8% yield). ^{1}H NMR (CD_3CN, δ): 1.49, 4H, t, 2,3-CH_2; 2.83, 6H, s, CH_3; 3.23, 4H, br, 1,4-CH_2; 6.66, 2H, br, NH; 6.95, 2H, d, H6′; 7.06, 2H, d, H5′; 7.56, 4H, t, H4; 7.90, 4H, t, H5; 8.04, 2H, d, H5″; 8.08, 4H, d, H3; 8.63, 2H, s, H3″; 8.68, 2H, s, H3′; 8.80, 4H, d, H6; 10.18, 2H, d, H6″. Anal. Calcd for $C_{52}H_{44}N_{12}Cl_2F_{12}O_2P_2Ru_2$: C, 43.62; H, 3.10; N, 11.74. Found: C, 43.88; H, 3.35; N, 11.39.

1,3-Xylenyldiamide/tppz Bridged Complex (5) (R = -CO-NH-CH$_2$-Ph-CH$_2$-NH-CO-). Eluting with toluene/acetonitrile (starting with 60% acetonitrile and increasing slowly to 100%) gave **5** (19% yield). ^{1}H NMR (CD_3CN, δ): 2.85, 6H, s, CH_3; 4.46, 4H, d, CH_2; 6.98, 2H, d, H6′; 7.16−7.24, 5H, m, H5′, H4−6^{Ph}; 7.30, 2H, t, NH; 7.42, 1H, s, H2^{Ph}; 7.55, 4H, t, H4; 7.91, 4H, t, H5; 8.04, 2H, d, H5″; 8.06, 4H, d, H3; 8.68, 2H, s, H3″; 8.70, 2H, s, H3′; 8.79, 4H, d, H6; 10.14, 2H, d, H6″. Anal. Calcd for $C_{56}H_{44}N_{12}Cl_2F_{12}O_2P_2Ru_2$: C, 45.45; H, 3.00; N, 11.36. Found: C, 45.62; H, 3.05; N, 11.26.

X-ray Crystallography. X-ray-quality crystals of *cis*-**2** were obtained by slow evaporation of a toluene/acetonitrile solution of the complex. A crystal of dimensions 0.15 mm × 0.15 mm × 0.40 mm was used for the structure determination. Cell dimensions were obtained from 8192 reflections, 2θ angle in the range 3−60 degrees and intensity data were collected by using a Bruker SMART diffractometer in the ψ scan mode. A total of 60 681 reflections were measured. Of the 10 844 unique reflections, 9119 had $I > 3\sigma$. Correction was made for absorption by using SADABS.

The structure was solved by direct methods with the NRCVAX system.[35] Non-hydrogen atoms were refined with anisotropic displacement parameters with the exception of the acetonitrile solvate, which, due to a slight unresolvable disorder, was refined isotropically and without disorder. Hydrogen atoms were included in calculated positions with isotropic displacement parameters 1.3 times the isotropic equivalent of the carrier carbon atoms.

Crystallographic data are listed in Table 1.

Table 1. Crystal Data for *cis*-[Cl(dmb)Ru(tppz)Ru(dmb)Cl](PF$_6$)$_2$, *cis*-**2**

formula	$C_{57}H_{51}Cl_2F_{12}N_{11}P_2Ru_2$
fw	1453.07
space group	$P2_1/n$
a (Å)	19.264(1)
b (Å)	11.6553(8)
c (Å)	27.951(2)
β (deg)	102.592(1)
V (Å^3)	6124.6(8)
Z	4
T (°C)	−100
D_{calc} (g cm^{-3})	1.576
μ (mm^{-1})	0.72
λ (Å)	0.710 73
$2\Theta_{max}$	50
no. of reflns collected	60 681
no. of unique reflns	10 844
no. of reflns with $I > 3\sigma$	9119
no. of parameters	761
R^a [$I > 3\sigma$]	0.053
$R_w{}^b$ (all data)	0.105

^{a} $R = \sum(|F_o - F_c|)/\sum(F_o)$. ^{b} $R_w = (\sum[w(|F_o - F_c|)^2]/\sum[w(F_o{}^2)])^{1/2}$.

Results

Syntheses. Ligands **6**−**8** were synthesized in good yield by reacting previously reported, derivatized bipyridines with commercially available dibromo- and diamino-containing starting materials. For **7** and **8** standard reagents were used for amide formation. As a result of the small changes observed in chemical shifts between reactants and products in **7** and **8**, the formation of the diamide was best confirmed by ^{1}H NMR in DMSO-d_6. In this solvent proton exchange is slow on the NMR time scale causing the amide proton to be observed as a triplet coupled to the adjacent methylene in each case.

Complex **1** was synthesized and purified by adsorption column chromatography on alumina. Impurities observed by chromatography included [Ru(tppz)(bpy)Cl]PF$_6$, identified by comparing the UV/vis spectrum to [Ru(tppz)(dmb)Cl]PF$_6$. The mononuclear complex eluted ahead of **1** and other products, possibly oligomeric in nature, were immobilized at the top of the column. ^{1}H NMR spectroscopy confirmed **1** to be a mixture of two isomers. The spectrum is complicated between 6.9 and 9 ppm and above 10 ppm there is a pair of doublets in a 3:2 ratio. These doublets correspond to the hydrogen atoms on each bpy most proximate to coordinated chloride. Similar low-field shifts have previously been observed,[31,36−38] and are attributable to a proximal effect of the chlorine to the pyridine hydrogen atoms in the 6-position of the ring. Due to symmetry across tppz in both isomers, one such resonance is expected for each consistent with an isomeric composition of 3:2.

A similar isomeric mixture was observed in the synthesis of **2**. Initial column chromatography separated **2** from impurities

(35) Gabe, E. J.; Le Page, Y.; Charland, J.-P., Lee, F. L.; White, P. S. *J. Appl. Crystallogr.* **1989**, *22*, 384.
(36) Zakeeruddin, S. M.; Nazeeruddin, M. K.; Pechy, P.; Rotzinger, F. P.; Humphry-Baker, R.; Kalyanasundaram, K.; Grätzel, M.; Shklover, V.; Haibach, T. *Inorg. Chem.* **1997**, *36*, 5937.
(37) Trammell, S. A.; Wimbish, J. C.; Obobel, F.; Gallagher, L. A.; Narula, P. N.; Meyer, T. J. *J. Am. Chem. Soc.* **1998**, *120*, 13248.
(38) Hartshorn, C. M.; Maxwell, K. A.; Meyer, T. J. Unpublished results.

Table 2. Selected Bond Distances (Å) and Angles (deg) for *cis*-[Cl(dmb)Ru(tppz)Ru(dmb)Cl]$(PF_6)_2$, *cis*-**2** (Numbering Scheme is Shown in Figure 2a)

Ru1−Cl1 2.398(1)	Ru1−N1 2.048(4)	Ru1−N14 2.089(4)
Ru1−N15 2.046(4)	Ru1−N22 1.944(3)	Ru1−N29 2.043(4)
Ru2−Cl2 2.391(1)	Ru2−N30 2.046(4)	Ru2−N37 1.955(3)
Ru2−N44 2.054(4)	Ru2−N45 2.041(4)	Ru2−N58 2.092(3)
Cl1−Ru1−N1 172.9(1)	Cl1−Ru1−N14 94.5(1)	Cl1−Ru1−N15 90.3(1)
Cl1−Ru1−N22 88.8(1)	Cl1−Ru1−N29 90.2(1)	N1−Ru1−N14 78.4(1)
N1−Ru1−N15 91.2(1)	N1−Ru1−N22 98.3(1)	N1−Ru1−N29 90.5(1)
N14−Ru1−N15 99.1(1)	N14−Ru1−N22 176.7(1)	N14−Ru1−N29 99.7(1)
N15−Ru1−N22 80.3(1)	N15−Ru1−N29 161.1(1)	N22−Ru1−N29 80.8(1)
Cl2−Ru2−N30 94.0(1)	Cl2−Ru2−N37 86.8(1)	Cl2−Ru2−N44 87.1(1)
Cl2−Ru2−N45 172.0(1)	Cl2−Ru2−N58 94.8(1)	N30−Ru2−N37 80.4(1)
N30−Ru2−N44 160.5(1)	N30−Ru2−N45 90.6(1)	N30−Ru2−N58 97.7(1)
N37−Ru2−N44 80.1(1)	N37−Ru2−N45 100.4(1)	N37−Ru2−N58 177.6(1)
N44−Ru2−N45 90.8(1)	N44−Ru2−N58 101.7(1)	N45−Ru2−N58 78.0(1)

analogous to those observed for **1**. Notably, less of the target complex remained adsorbed on the column. Consequently, alumina chromatography on a small quantity of the isolated complex with slow elution allowed for separation of *trans*-**2** and *cis*-**2**. This was confirmed by ^{1}H NMR spectroscopy and the appearance of only one resonance in the 10 ppm region for each isomer collected. Due to the symmetries of the isomers it was not possible to assign the two isomers by ^{1}H NMR. A single-crystal X-ray structure determination of the minor, more slowly eluting isomer was carried out in order to accomplish this and the structure, discussed in more detail below, proved this isolated isomer to be *cis*-**2**.

The synthesis of complexes **3**−**5** are similar to those of **1** and **2** although the reactions were carried out at lower concentrations in order to favor the monomeric cis isomer over oligomeric products. A greater amount of immobilized material remains adsorbed during chromatographic purification of these complexes. In the ^{1}H NMR spectra of **3**−**5** only one resonance is observed above 10 ppm as was also observed for isolated *trans*-**2** and *cis*-**2**, thus confirming the isolation of a single isomer in each case.

For the five complexes **1**−**5** varying amounts of the product mixture remain adsorbed on the column thus reducing the overall yield. This has also been a significant problem for previously reported tppz complexes.[28]

X-ray Crystallography. The minor isomer of **2** crystallizes in the monoclinic space group $P2_1/n$ and contains one dinuclear tppz molecule, two hexafluorophosphate anions, and toluene and acetonitrile solvates in the asymmetric unit. Perspective views and atom labeling of the dinuclear unit are shown in Figure 2, and a list of selected bond lengths and angles is given in Table 2.

The complex is shown by this structure to be the cis isomer of **2**. There is significant distortion away from octahedral geometry at each ruthenium and a distortion away from planarity in the bridging ligand, particularly in the pyrazine ring. In examining these features it is useful to compare them to previously reported structures: the mononuclear analogue, [Ru(tppz)(dmb)Cl]PF_6;[31] other pyrazine-bridged ruthenium dimers;[39,40] and the only other previously reported structure of a dinuclear tppz complex, $[(H_2O)_2Cu(tppz)Cu(H_2O)_2](ClO_4)_4\cdot 2H_2O$.[41]

The distortion from octahedral geometry around the ruthenium atoms is similar to that observed in the mononuclear complex. Meridional coordination of tppz leads to trans pyridyl coordination angles of 160.5(1)° and 161.1(1)° compared to 159.4° for the earlier structure. This slight increase in angle results from a slight decrease in Ru−N(pz) distance in the dimer (1.944(3) and 1.955(3) Å compared to 1.962 Å). A similar effect has previously been observed in comparing mono- and dinuclear ruthenium complexes of pyrazine and has been attributed to an increased extent of $d\pi(Ru^{II}) \rightarrow \pi^*$(pz) back-bonding which provides a basis for electronic coupling through the pyrazine bridge.[40]

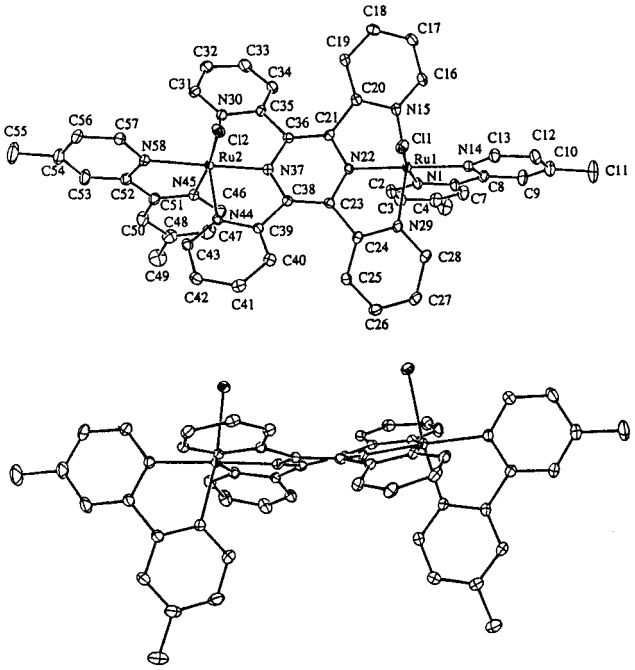

Figure 2. (a) Perspective view and atom labeling of the X-ray crystal structure of *cis*-**2**·$PhCH_3$·CH_3CN. The hydrogen atoms, hexafluorophosphate anions and solvate molecules have been omitted for clarity. (b) Perspective view showing the disposition of the ruthenium coordination spheres.

There is considerable distortion from planarity in the pyrazine ring (Figure 2b, max. dev. 0.096(6) Å). This distortion is similar to that in the analogous mononuclear complex (max. dev. 0.11 Å) and in other mononuclear tppz complexes.[42] This is somewhat surprising since it could be anticipated that upon coordination of a second ruthenium, greater steric crowding between the hydrogen atoms in the 3-position of the pyridyl rings might result in increased nonplanarity in the pyrazine ring. However, in the previously reported dinuclear copper complex, the pyrazine ring has crystallographically imposed planarity. In

(39) Fürholz, U.; Joss, S.; Bürgi, H. B.; Ludi, A. *Inorg. Chem.* **1985**, *24*, 943.
(40) Coe, B. J.; Meyer, T. J.; White, P. S. *Inorg. Chem.* **1995**, *34*, 593.
(41) Graf, M.; Greaves, B.; Stoeckli-Evans, H. *Inorg. Chim. Acta* **1993**, *204*, 239.
(42) Vogler, L. M.; Scott, B.; Brewer, K. J. *Inorg. Chem.* **1993**, *32*, 898.

Table 3. Electrochemical and UV−Visible Data for **1**−**5**

	$E_{1/2}$ (in CH_3CN vs SSCE, scan rate 100 mV s^{-1})						MLCT λ_{max} (nm) (ϵ (10^4 dm^3 mol^{-1} cm^{-1})) in CH_3CN	
	Ru^{III}/Ru^{II}		ligand reduction					
complex	$E_{1/2}(1)$	$E_{1/2}(2)$					Ru(dπ) → tppz(π*)	Ru(dπ) → bpy(π*)
$[(Cl(bpy)Ru)_2(tppz)]^{2+}$, **1**	0.96	1.25	-0.60	-1.10	-1.79[a]		598 (3.03)	436 (1.54)
$[(Cl(dmb)Ru)_2(tppz)]^{2+}$, **2**	0.91	1.20	-0.62	-1.12	-1.84[a]		604 (2.93)	434 (1.52)
$[Cl(NN)Ru(tppz)Ru(NN)Cl]^{2+}$, **3** (ether)	0.92	1.26	-0.55	-1.07	-1.67	-1.75	616 (2.86)	434 (1.54)
$[Cl(NN)Ru(tppz)Ru(NN)Cl]^{2+}$, **4** (butyl diamide)	0.99	1.34	-0.50	-0.99	-1.51	-1.60	622 (2.94)	444 (1.46)
$[Cl(NN)Ru(tppz)Ru(NN)Cl]^{2+}$, **5** (phenyl diamide)	0.99	1.33	-0.50	-1.00	-1.54	-1.62	624 (2.87)	442 (1.45)

[a] Irreversible, $E_{p,c}$ reported.

the present structure, the pyrazine ring is twist-boat distorted. This is most clearly seen in the displacement of the four carbon substituents from the plane of the pyrazine ring (average displacements: C24/C35 0.370(4) Å; C20/C39 0.436(4) Å).

The intramolecular Ru···Ru separation is 6.558(1) Å, a distance considerably shorter than in other pyrazine-bridged ruthenium dimers (6.85−7.00 Å). This is due to both the shorter Ru−N(pz) bonds in *cis*-**2** as a result of tppz coordination and the distortion in the pyrazine portion of the ligand.

The pyridine ring disposition of the two halves of the complex and the coordinated half of the mononuclear complex are similar. Each half-tppz has a pyridine ring with a smaller dihedral angle with the pyrazine (*cis*-**2**, 16.1°, 17.1°; mononuclear complex, 15.1°) and a larger angle (23.5°, 24.8°; 22.6°). The angle between the two pyridine rings is also similar (8.0°, 11.7°; 11.4°). The four pyridines of *cis*-**2** are arranged in an alternating pattern around the pyrazine ring to minimize steric strain. The side view in Figure 2b shows that the dmb rings are distorted away from each other. This results in a rotation of the Ru coordination spheres with respect to the pyrazine unit. The cis N(pz)−N(dmb) angles are large (98.3(1)°, 100.4(1)°), and the trans N(pz)−N(dmb) angles (176.7(1)°, 177.6(1)°) are closer to 180° than is observed in related structures. The N(pz)−Cl angles are acute (88.8(1)°, 86.8(1)°). This is possibly due to steric repulsion of the dmb hydrogen atoms on C2 and C46 away from the pyrazine ring. Similar, although smaller, effects can be seen in $[Ru(tpy)(bpy)X]^{n+}$-type complexes (X = NCS, $NCCH_3$, H_2O) provided that X is small and does not introduce off-setting steric effects.[36,43,44] A result of these steric effects is a relatively short intramolecular Cl···Cl distance of only 5.880(2) Å. This could be an important structural feature in the cooperative reactivity of related aqua/oxo complexes.

^{1}H NMR Spectroscopy. While the NMR resonances are typically sharp and well resolved, broadening is observed for **3**−**5**, in particular for H3(tppz) (at 8.08 ppm) and, to a lesser extent, for H4(tppz) (7.54 ppm) (Figure 3). As seen in the crystal structure of *cis*-**2**, there is significant steric crowding in this region for dinuclear tppz complexes. The broadening observed results from rapid exchange between two hydrogen environments, one distorted toward the proximate Cl, the other, distorted away. This dynamic phenomenon is observed for the strapped complexes but not for **1** and **2**. Presumably for **3**−**5** the attached bipyridine bridge also requires reorganization, thereby slowing down the interconversion.

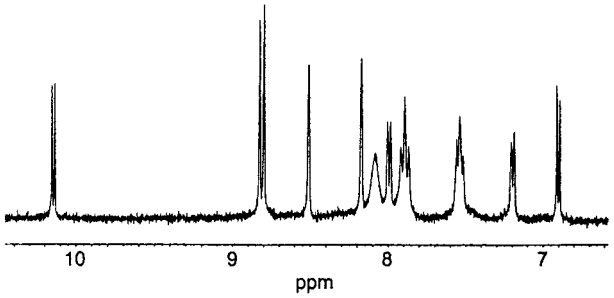

Figure 3. ^{1}H NMR spectrum of **3**.

Electrochemistry. Results of electrochemical measurements on **1**−**5** are presented in Table 3. For each, two reversible $Ru^{III/II}$ oxidations are observed. The first potential ranges from 0.91 V (vs SSCE) for the dmb complex, **2**, to 0.99 V for the amide-containing complexes **4** and **5**. A range of potentials is also observed for the second oxidations with **2** having the lowest potential (1.20 V) and **4** and **5** the highest (1.34 and 1.33 V, respectively). The three complexes with strapped bpy's have consistently higher $\Delta E_{1/2}$ ($= E_{1/2}(2) - E_{1/2}(1)$) values than **1**.

For the five complexes there are two reversible one-electron reductions: the first is between −0.50 and −0.62 V and the second is between −0.99 and −1.12 V vs SSCE. This has been observed in previously reported dinuclear tppz complexes,[28−30] although at less negative potentials, and assigned to sequential, tppz-based reductions.

At more negative potentials, further reductions are observed. For **1**, there is an irreversible reduction at −1.79 V with new features appearing upon scanning in the reverse direction at −0.44 and −0.93 V. For **3**−**5**, the new features are smaller and two reversible reductions are observed. These are observed at less negative potentials for the amide-linked complexes **4** and **5** than for ether-linked **3**. These observations are consistent with bpy-based reductions with reduction leading to Cl^-

(43) Soek, W. K. Ph.D. Thesis, University of North Carolina, Chapel Hill, NC, 1988.
(44) Rasmussen, S. C.; Ronco, S. E.; Mlsna, D. A.; Billadeau, M. A.; Pennington, W. T.; Kolis, J. W.; Peterson, J. D. *Inorg. Chem.* **1995**, *34*, 821.

Scheme 1

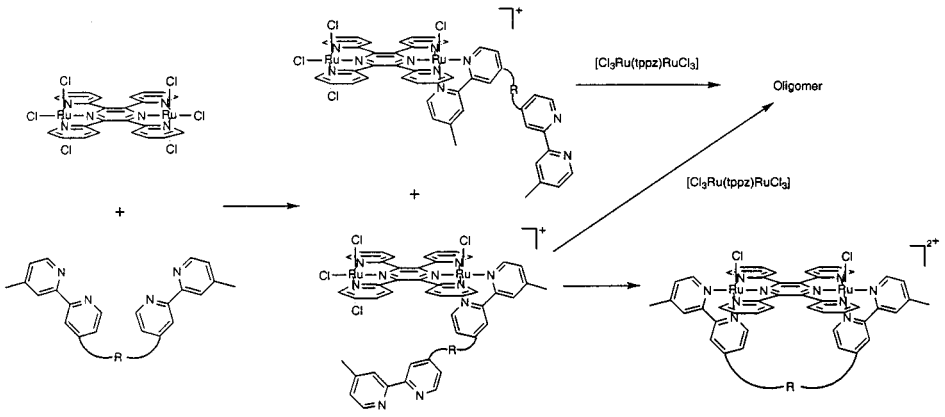

substitution by CH_3CN. Interestingly, in the bridged complexes distinct bpy reductions are observed with $\Delta E_{1/2}$ between 80 and 90 mV consistent with electronic interaction between the ligands through the $Ru^{II}(tppz^{2-})Ru^{II}$ bridge.

UV−Visible Spectroscopy. Spectroscopic data for **1**−**5** are presented in Table 3. The UV bands arise from ligand-based $\pi-\pi^*$ transitions. The visible bands originate from metal-to-ligand charge transfer (MLCT) with $Ru(d\pi) \rightarrow bpy(\pi^*)$ at 434−444 nm and $Ru(d\pi) \rightarrow tppz(\pi^*)$ at 600−624 nm. The shift to lower energy of these bands for **4** and **5** parallels the difference in $E_{1/2}(Ru^{III/II})$ and the first ligand reduction as expected.

Discussion

Syntheses. The key synthetic advances in this work will become important in later investigations of the mixed-valence forms of these complexes and of cooperative effects in the redox chemistry of $Ru^{II}-OH_2^{2+}/Ru^{IV}=O^{2+}$ complexes to which the chloro complexes are precursors. In utilizing tppz as a bridging ligand in the latter studies, it will be important to compare reactivities of the cis and trans isomers. In the trans isomer the two oxidizing sites will be too remote from each other for simultaneous reaction with a single substrate molecule. Because of this, attempts were made to separate the isomeric mixtures of **1** and **2**. Attempts to separate the isomers were focused on **2** since product loss due to adsorption on the column was less significant in this case. Separation was achieved on a small scale over considerable elution times and isomeric assignment was only possible through X-ray crystal structure determination.

A selective approach to the selective preparation of cis isomers was investigated here in which two bpy groups are linked together by a bridge. This approach gave the desired cis isomers without the small scale, time-consuming chromatographic methods required for isomeric separation of **2**. To be successful, the bridge must be long enough to allow the bpy's to coordinate to the two ruthenium atoms separated by ∼6.6 Å. Longer or shorter bridge lengths which do not span the metal ions will favor the formation of oligomeric products in which the bridged bpy units coordinate to ruthenium ions of different $[Cl_3Ru(tppz)RuCl_3]$ units. A sufficiently long bridge length could also conceivably span the coordination positions of the trans isomer.

Initially the ether-linked ligand **6** was synthesized which contains an eight-atom bridge between the bpy groups. The reaction between $[Cl_3Ru(tppz)RuCl_3]$ and this ligand under reducing conditions gave the desired cis isomer, **3**, in a yield significantly lower than that for **1** under the same conditions (18% and 57%, respectively). This is not unexpected since (i) initial coordination of the bridge-substituted pyridine in a trans position to the pyrazine presumably leads to oligomeric products; and (ii) even on coordination of this pyridine in the desired cis site, there remains competition between monomer and oligomer formation (Scheme 1).

Given our interest in future investigations of $Ru^{IV}=O$ reactivity based on these complexes as precursors, a bridge is required between bpy groups that will be unreactive toward this oxidant. Ether groups are oxidized to the corresponding carboxylic esters by RuO_4 and ether oxidation chemistry by *cis*-$[Ru^{IV}(bpy)_2(py)(O)]^{2+}$ has also been reported.[43] To reduce the possibility of bridge-oxidizing side reactions, an eight-atom amide-containing bridge, **7**, was also prepared. The yield of strapped complex **4** from the reaction between this ligand and $[Cl_3Ru(tppz)RuCl_3]$ was only 8%. The reduced yield is presumably attributable to less favorable conformational requirements in competition with oligomer formation. The planar amide groups in **7** provide less conformational freedom than in **6**, and this apparently reduces the ease with which the two ruthenium atoms can be bridged.

In an attempt to increase yield, the nine-atom diamide bridge was synthesized and allowed to react with $[Cl_3Ru(tppz)RuCl_3]$ which gave **5** in 19% yield which approached the ∼23% overall yield of *cis*-**1**. These results suggest that with an appropriate choice of bridging ligand and reaction conditions, it is possible to achieve reasonable yields of the *cis*-strapped complexes.

Structure and Properties. There are some key features in the structure of *cis*-**2** which may be of relevance in future studies. One is the metal−metal separation distance. For pyrazine-bridged ruthenium dimers this distance is 7 Å, a value that has been used in calculations for tppz bridges.[30] The actual distance in *cis*-**2** is 6.55 Å which is less by 7%. In the studies of comparative reactivity, an important molecular parameter is the distance between the Ru−Cl sites. Because of the distortion in the tppz bridge in the structure of *cis*-**2**, the Cl···Cl distance is only 5.880(2) Å, a significantly shorter distance than the expected 7 Å for pyrazine-bridged complexes. If this distance is maintained in the analogous bridged dioxo complexes, it will influence the separation distance between reactive functional groups that are accessible for potential four electron oxidation.

The order of $E_{1/2}(1)$ values for the $Ru^{III/II}$ couples in **1**−**5** is consistent with the substituents on the coordinated bipyridine (see Table 3). Relative to **1**, the lower $E_{1/2}(1)$ values for **2** and **3**, the dmb and ether-linked dimers, are consistent with the presence of the electron donating alkyl groups. The values for $E_{1/2}(1)$ for amide-bridged dimers **4** and **5** are increased due to the electron withdrawing amide substituents. The $E_{1/2}(1)$ value

for **2** is the same as that for the analogous mononuclear complex, an observation made for other monomer/dimer comparisons. The $E_{1/2}(1)$ value for **1** (0.96 V vs SSCE) is greater than in the related dimer *cis*,*cis*-$[(bpy)_2ClRu(pz)RuCl(bpy)_2]^{2+}$ (0.89 V), consistent with extensive Ru(dπ) → tppz(π^*) back-bonding.

The $\Delta E_{1/2}$ values ($= E_{1/2}(2) - E_{1/2}(1)$) for **1**−**5** vary from 290 mV for **1** and **2** to 340−350 mV for the bridged-bpy complexes **3**−**5**. Surprisingly, there is no evidence for separate Ru^{III}/Ru^{II} couples for the cis/trans isomers of **1** and **2**. We are forced to conclude that the voltammetric waves for their couples completely overlap and that the $E_{1/2}$ values are the same.

The magnitudes of the $\Delta E_{1/2}$ values are considerably greater than for *cis*,*cis*-$[Cl(bpy)_2Ru(pz)Ru(bpy)_2Cl]^{2+}$ (120 mV).[45] For the comproportionation equilibrium in eq 2, $\Delta E_{1/2} = -\Delta G^\circ_{com}$.

$$Ru^{II}-Ru^{II} + Ru^{III}-Ru^{III} \rightarrow Ru^{III}-Ru^{II} \qquad (2)$$

In earlier work the factors influencing the magnitude of ΔG°_{com} have been identified as (1) a statistical effect which favors the mixed-valence $Ru^{III}-Ru^{II}$ form, (2) an electrostatic effect which also favors the mixed-valence ion, and (3) electronic delocalization.[46] Given the similarity in charge types between *cis*,*cis*-$[Cl(bpy)_2Ru^{III}(pz)Ru^{II}(bpy)_2Cl]^{3+}$ and the tppz dimer, the first two factors should be comparable, and electronic delocalization must play an important role in dictating the magnitude of $\Delta E_{1/2}$ in the tppz dimer. The mixed-valence forms are currently under investigation.

Acknowledgments are made to the National Science Foundation (Grant No. CHE-9321413), the U.S. Department of Energy (Grant No. DE-FG02-96ER 14607) and Proyecto Fondecyt, Lineas Complementarias 8980007, and Proyecto Fondecyt 1940577.

Supporting Information Available: Listings of information containing atom coordinates, anisotropic displacement parameters and a complete list of bond distances, bond angles, and torsion angles for *cis*-**2**; UV−visible spectrum of **1**, representative of the five complexes; and ^1H NMR spectra of *cis*- and *trans*-**2**. This material is available free of charge via the Internet at http://pubs.acs.org.

IC990110A

(45) Callahan, R. W.; Keene, F. R.; Meyer, T. J.; Salmon, D. J. *J. Am. Chem. Soc.* **1977**, *99*, 1064.

(46) Richardson, D. E.; Taube, H. *Coord. Chem. Rev.* **1984**, *60*, 107.